# Analysis of Different SAR Polarimetric Decomposition Methods using EOS-04 Polarimetric Data for Urban and Natural Features

**Srivally MV*, Sujata Ghosh, Nidhi Chaubey, Swati Upadhyay, & Sumit Pandey**

[1]Advanced Data Processing Research Institute (ADRIN), Department of Space, Govt. of India, Secunderabad, India
*Corresponding Author's email: srivally@adrin.res.in

**Abstract**

The all-weather imaging capability and unique sensitivity towards the geometrical and structural properties of the object makes Synthetic Aperture Radar (SAR) data best suited for monitoring of various land cover objects and extraction of object parameters. SAR imagery has certain characteristics, patterns and features which can be used for information extraction of both urban objects and natural features. Polarimetric Synthetic Aperture Radar records Polarimetric information and hence become sensitive to orientation and characteristics of the object. It has the potential to yield several new parameters for object detection and hence this technique is utilized extensively for image classification. In this paper, various Polarimetric decomposition methods are applied and compared for different polarized data namely Circular, Dual and Full-pol polarization acquired from Earth Observation Satellite-04 (EOS-04). M-Chi, M-Delta, M-Alpha and Pauli, Sinclair and Freeman-Durden Polarimetric decomposition methods are used to generate decomposed outputs on different test areas covering different terrain types like urban, vegetation and water situated at different locations over the Earth for information extraction of natural and man-made objects on Earth surface from EOS-04 data. These decomposition methods were implemented in-house developed ShARP+ (Synthetic Aperture Radar Processor Plus) software. Objective of this paper is to compare the results among many coherent and incoherent Polarimetric decomposition methods in differentiating the objects on the ground to assess its potential for classification of surface features. The results and analysis are presented in the paper.

**Keywords** SAR; EOS-04; Polarization; Polarimetric Decomposition

## Introduction

Optical Remote Sensing data is vulnerable to foggy, rainy and snowy weathers, which jeopardizes the access of high-quality and continuous data. Synthetic Aperture Radar (SAR) Remote Sensing can work all day and adapt to various weathers. SAR has the ability to penetrate various objects on the ground. It can not only obtain the surface information of objects, but also reflect the internal structure information. Microwave Remote Sensing for extracting urban information and natural features is completely different from optical sensors.

Polarimetric SAR data provides a scattering matrix of a terrain's surface. The scattering matrix consists of magnitude and phase at polarizations (HH/HV/VH/VV), that are sent and receive horizontally (H)- and vertically (V)-polarized waves by SAR antenna. Advantage of using Circular, Dual and Full-pol Polarimetric SAR data could extract the Polarization matrix, geometric structure, dielectric constant and other information of ground-objects. Polarization decomposition method could effectively extract the scattering characteristics of the object.

Polarization decomposition technology is widely used for Remote Sensing image classification. Some methods have been suggested in order to obtain earth surface characteristics from different Polarization (Circular, Dual and Full-pol) data. Wei et al. (2017)

proposed a multi-component decomposition method for Polarimetric SAR data by combining the Generalized Similarity Parameter (GSP) and the eigenvalue decomposition [1]. The usefulness of Polarimetric decomposition methods for LULC mapping of ALOS L-band PolSAR using Freeman-Durden and Yamaguchi decomposition methods was examined by Bikash Ranjan Paridal et al. (2020) [2]. Three-Component Model-Based Decomposition for Polarimetric SAR Data was presented by Wentao An et al. [5]. Exploring the Capability of Compact Polarimetric (Hybrid Pol) C Band
RISAT-1 Data for Land Cover Classification was presented by Kiran Dasari et al. (2018) [15] and some of the techniques were applied to assessment applications.

In this study, Circular (RH, RV), Dual (HH, HV) and Full-pol (HH, HV, VH, VV) Polarization data is acquired at Fine Resolution Strip Map Mode-1 (FRS-1) have been used. These products are processed at Level-1 SLC (Single Look Complex) and in CEOS (Committee on Earth Observation Satellites) image format. In this paper work, systematically compared the classification performance between different Polarization decomposition methods applied on Polarimetric SAR data [10]. Our emphasis is on the inter-comparisons among classification results based on different Polarimetric decomposition methods (M-Chi, M-Delta, M-Alpha for Circular Polarimetry and Freeman–Durden, Sinclair and Pauli decomposition for Linear Polarimetry).

Due to the high variability of urban landscape, its complex combinations of natural and man-made objects, and object forms and sizes, the scattering mechanisms are much more complex in built-up area when compared with natural targets. The three types of scattering mechanisms possible in ground are i) even, ii) volume and iii) odd bounce. Polarimetric decomposition of Polarimetric SAR data is essential to understand the predominant scattering type. Building orientation with respect to the SAR sensor look direction has a critical influence on the interpretation of Polarimetric Synthetic Aperture Radar data in urban areas. In this paper, the effect of orientation of the object also analyzed on scattering mechanisms in different decompositions. The structure of this paper is as follows: Section 2 introduces the study area. Section 3 presents Materials and the Polarimetric SAR decomposition principles, Methods and Section 4 presents the Polarimetric decomposition results and analysis of the different terrain features, object classification and the discussion, respectively. Finally, the conclusions and future research topics are presented in Section 5.

**Materials and Methods**

*Study Area:* In this paper four datasets are used to analyze the performance of different Polarimetric decomposition methods. First study area is an agricultural area located in Rajasthan state, India. Second study area is covering part of Visakhapatnam city in Andhra Pradesh State, Southern India. This study area comprises the well forested Eastern Ghats (vegetation), coast of the Bay of Bengal (water area) and urban structures. Third study site is Shadnagar town located in the Indian state of Telangana. This dataset consists of vegetation and urban structures (roads and settlements). Fourth study area is located in San Francisco, CA, USA, which has coverage of built-up areas with different orientations, forests and oceans.

*Datasets:* In this paper, the major datasets covering above mentioned study areas are acquired from space borne system EOS-04 and the Circular pol data is acquired from RISAT-1 satellite. These datasets are having different terrain types like urban settlements, vegetation areas and waterbody regions. In this study, Level-1 SLC products are used for generating Polarimetric decomposed products of various decomposed methods. We have used one dataset of Circular, one dataset of Dual and two datasets of Full-pol data for analysis.

*Materials:* The major advantage of Polarimetric SAR data is the utilization of backscatter coefficients that strongly depends on the scattering properties of ground object. The Polarimetric SAR data is acquired from EOS-04, which is an indigenous satellite, launched on

14, Feb 2022 by ISRO's Polar Satellite Launch Vehicle (PSLV) C-52. SAR sensor of EOS-04 is capable of providing data in various resolution modes catering to a variety of applications to the users. The SAR payload of EOS-04 will be operating in C-band at a frequency of 5.4 GHz and imaging in Side-Looking Radar mode. The EOS-04 SAR system has been designed to provide Single, Dual, Full-pol, Hybrid Circular Polarimetry (Transmit circular, receive linear) data for FRS-1, FRS-2 and for Medium Resolution ScanSAR Mode (MRS) and Coarse Resolution ScanSAR Mode (CRS). For this study, we used Level-1, SLC data products in CEOS format of Single, Dual, Circular, Full pol data for analysis. These data sets are indented and downloaded through Bhoonidhi web portal [17]. The SLC data is processed and decomposed outputs are generated through in-house developed ShARP+ software.

In the present study, Linear (Pauli, Sinclair and Freeman-Durden) and Circular (M-Chi, M-Delta and M-Alpha) Polarimetric decomposed outputs are generated. The analysis of these decomposed outputs is done and also the thematic classes, such as urban built-up area, vegetation like plantation, crop area, forest region and waterbody are generated using Supervised Classification technique (Support Vector Machine (SVM) classifier) to assess the potential of decomposed outputs in discriminating the ground features.

*Methodology:*

*Pre-processing of SLC data*

*Importing the data:* Different Polarization (Circular, Dual and Full-pol) data is imported into in-house developed ShARP+ software using import module (Figure 1).

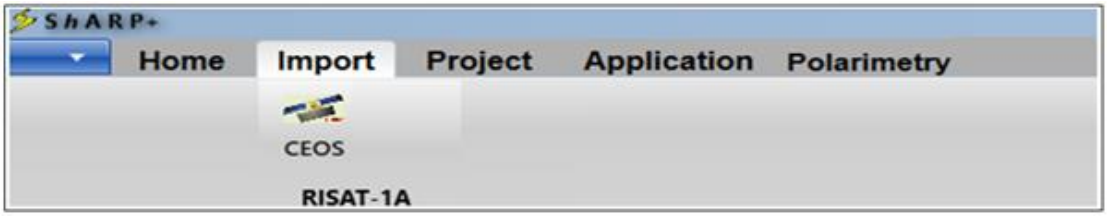


**Fig. 1** SLC data import module of of ShARP+ software.

Real (I channel) and Imaginary (Q channel) data of each Polarization, corresponding parameters file (.ppr) and project file (.asp) is generated. Here each parameters file (.ppr) contains meta information of each Polarization data and project file (.asp) comprises the project details and information of SLC products. These files are used as input for Polarimetric decomposition process. Polarimetric decomposition is mainly classified into two types. One is Coherent decomposition (Pauli and Sinclair) based on Scattering Matrix S shown in Eq. (1) and another one is Model based decomposition (Freeman-Durden) based on Coherency (T3) and Covariance (C3) matrix.

$$\text{Scattering Matrix } [S] = \begin{bmatrix} S_{hh} & S_{hv} \\ S_{vh} & S_{vv} \end{bmatrix} \quad (1)$$

*Decomposition modules in ShARP+ software:* Decompositions allow the separation of different scattering contributions and can be used to describe the scattering properties (geometry and intensity) of the objects on the ground. In this paper, various decomposed outputs are generated using Decomposition modules of ShARP+ software. This software is designed as standalone software for processing, analysis and exploitation of Polarimetric SAR data. Various Decomposition modules of different Polarization (Circular, Dual and Full-pol) data are implemented in-house developed ShARP+ software (Figure 2).

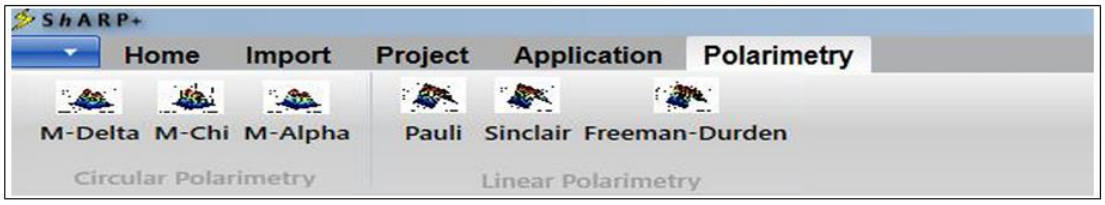


**Fig. 2** Polarimetry data decomposition modules of ShARP+ software.

*Coherent Decomposition:* Scattering matrix [S] plays an important role in Coherent decomposition. Coherent decomposition generates based on the Scattering matrix [S] (Eq. (1)) and the Scattering matrix is able to characterize coherent scatterers. In this paper, Pauli and Sinclair Coherent decomposition techniques are used to generate decomposed products. These Polarimetric decompositions (Pauli and Sinclair) are suitable for the detection of natural targets.

The (R, G, B) bands produced by the Pauli decomposition correspond to the following intensities:

- Red: $0.5*|S_{hh} - S_{vv}|^2$, which represents the power scattered by objects characterized by double or even bounce.
- Green: $0.5*|S_{hv} + S_{vh}|^2$, which represents the scatter power by objects that are able to return the orthogonal polarization, for example the volume scattering produced by the forest canopy.
- Blue: $0.5*|S_{hh} + S_{vv}|^2$, which represents the contribution of single or odd bounce scattering to the final measured scattering matrix.

The Sinclair decomposition produces (R, G, B) bands with the following intensities:
Red: $|S_{vv}|^2$, Green: $|(S_{hv} + S_{vh})/2|^2$, Blue: $|S_{hh}|^2$

*Incoherent Decomposition*

Most of the objects on the earth surface are heterogeneously scattered, therefore incoherent decomposition provides the best results in identify such objects. For Full-pol data analysis, we attempted a three-component Polarimetric decomposition technique called Freeman–Durden Decomposition [5]. The Freeman decomposition is a Model based decomposition that models the Coherency matrix (T) as the contribution of three scattering mechanisms namely canopy, even or double bounce and Bragg scattering mechanisms. Canopy scatter from a cloud of randomly oriented dipoles. Even bounce scatter from a pair of orthogonal surfaces with different dielectric constants. Bragg scatters from a moderately rough surface. The power scattered by the components of the Coherency matrix (T) of the above three scattering mechanisms are employed to generate a RGB (double-bounce, volume-scattering, surface-like scattering) image. In a Polarimetric SAR image, each pixel is represented by a Coherency Matrix T, which is a 3 × 3 nonnegative definite Hermitian matrix is mentioned below:

$$T = \begin{bmatrix} T_{11} & T_{12} & T_{13} \\ T^*_{12} & T_{22} & T_{23} \\ T^*_{13} & T^*_{23} & T_{33} \end{bmatrix} \qquad (2)$$

Where the superscript $*$ denotes the conjugate. The three scattering mechanisms, surface, double-bounce, and volume scatterings of Freeman–Durden decomposition method can be expressed as follows:

$$T = P_s T_{surface} + P_d T_{double} + P_v T_{volume} \qquad (3)$$

Where Ps, Pd, and Pv correspond to the power of each scattering component and their sum is equal to Span.

$$\text{Span} = P_s + P_d + P_v = T_{11} + T_{22} + T_{33} \quad (4)$$

The following Figure 3 represents the flow chart of three-component Polarimetric decomposition technique (Freeman-Durden) used in this study.

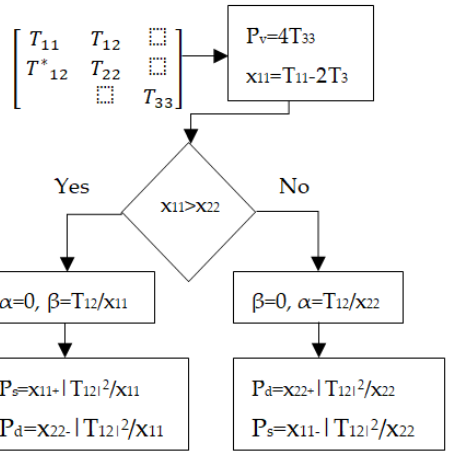


**Fig. 3** Flowchart of the Freeman-Durden decomposition generation program.

The below Figure 4 shows the implementation flowchart for generating Full-pol Polarimetric data decomposed outputs using different decomposition techniques.

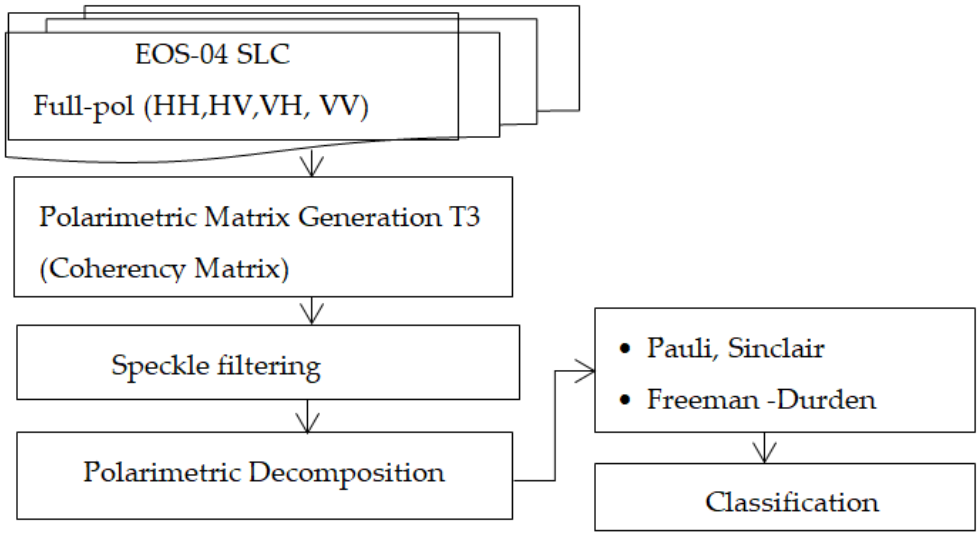


**Fig. 4** Flowchart of the proposed work for generating Full-pol data decomposed products.

*Circular Polarization Decomposition:* Circular Polarimetry is transmitting a circular polarization and receiving in linear polarization. In this paper, we assess the performance of Circular Polarimetry for extracting urban and natural features from various ground objects. This has done based on Stokes parameters namely, Degree of Polarization (DoP), Circular Polarization Ratio (CPR), Scattering Mechanism, Degree of Circularity and Relative Phase values [15]. These parameters are derived from Stokes vector. Stokes vector is a set of values

which describes the Polarization state of electromagnetic signal. The four Stokes Vector values from the backscattered signal are represented in the form of matrix as follows:

$$\begin{bmatrix} S0 \\ S1 \\ S2 \\ S3 \end{bmatrix} = \begin{bmatrix} < |E_{RH}|^2 > + < |E_{RV}|^2 > \\ < |E_{RH}|^2 > - < |E_{RV}|^2 > \\ 2Re < E_{RH}.E^*_{RV} > \\ -2Im < E_{RH}.E^*_{RV} > \end{bmatrix} \quad (5)$$

From the Eq. (5) $E_{RH}$ represents signal received by the channel with right circular transmit and horizontal (linear) receive. Correspondingly $E_{RV}$ represents signal received by the channel with right circular transmit and vertical (linear) receive.

In order to understand the scattering mechanism of ground objects, M-Delta (m-δ), M-Chi (m-χ) and M-Alpha (m-α) decomposition methods are performed on Circular Polarimetry datasets [3]. Flowchart of the proposed work for generating Circular Pol data decomposed outputs is shown in Figure.5.

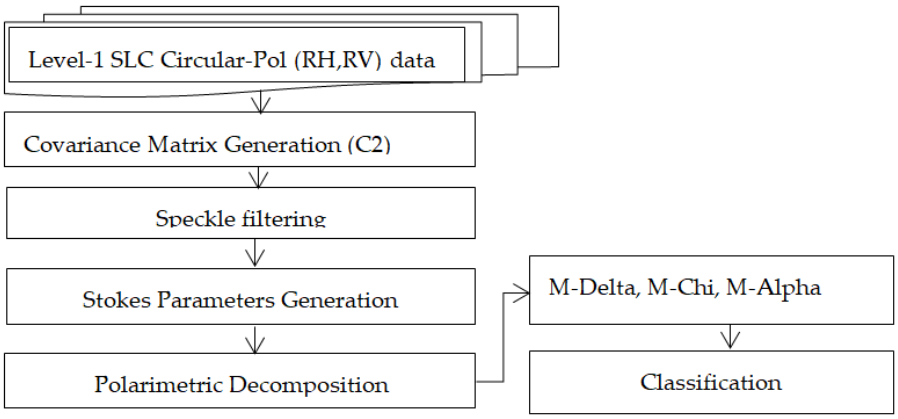


**Fig. 5** Flowchart of the proposed work for generating Circular pol data decomposed products.

*M-Delta(m-δ) Decomposition:* The M-Delta decomposition comprises of Degree of Polarization (m) and Relative Phase (δ). In this decomposition technique, m is the sensitive indicator of volume scattering and δ is the sensitive indicator of even bounce against odd bounce scattering [3]. In this decomposition, red represents even bounce, green represents volume component, and blue represents the odd bounce as shown in Eq. (6).

$$\text{B=odd bounce=f}_{\text{odd}} = \sqrt{S0 * m * \frac{1+sin\delta}{2}}$$

$$\text{R=even bounce=f}_{\text{even}} = \sqrt{S0 * m * \frac{1-sin\delta}{2}}$$

$$\text{G=diffused bounce=f}_{\text{diffused}} = \sqrt{S0 * (1-m)} \quad (6)$$

Where S0 is stokes vector value shown in Eq.(5).

*M-Chi (m-χ) Decomposition*

M-Chi decomposition is calculated using the Stokes Vector values S0 and S3 (Eq. (5)), and the degree of polarization (m) as shown in Eq. (7). M-Chi decomposition can be expressed in RGB image where

$$\text{B=odd bounce=f}_{\text{odd}} = \sqrt{S0 * m * \frac{1+sin2\chi}{2}}$$

$$\text{R=even bounce=f}_{\text{even=}}\sqrt{S0 * m * \frac{1-sin2\chi}{2}}$$

$$\text{G=diffused bounce=f}_{\text{diffused=}}\sqrt{\text{S0} * (1 - \text{m})} \quad (7)$$

Here S0 is stokes vector value shown in Eq. (5).

*M-Alpha (m-$\alpha$) decomposition*

M-Alpha decomposition comprises of Degree of Polarization (m) and Polarization angle ($\alpha$) as shown in Eq. (8). This parameter can be estimated from Circular Polrimetric SAR data when there is dominant scattering from urban and agriculture fields.

$$\text{B=odd bounce=f}_{\text{odd =}}\sqrt{S0 * m * \frac{1-cos2\alpha}{2}}$$

$$\text{R=even bounce=f}_{\text{even=}}\sqrt{S0 * m * \frac{1+cos2\alpha}{2}}$$

$$\text{G=diffused bounce=f}_{\text{diffused=}}\sqrt{S0 * (1 - m)} \quad (8)$$

Here S0 is stokes vector value shown in Eq. (5).

*Supervised Classification:* Support Vector Machine (SVM) classifier: SVM is used on images to identify the class associated with each pixel. It provides good classification results from complex and noisy data. This classification method separates the classes with a decision surface that maximizes the margin between the classes and classification provides a process that improves performance without significantly degrading results [4]. It is most effective when operating in areas that contain homogenous features, such as water bodies and fields.

In this paper, we collected training samples and selected polygons mentioned in Table 1 and 3 for different classes (water, vegetation and urban) to classify the study areas one and two (Figure 6 and 7). These training samples are delineated as image objects in classification.

After training sample generation, SVM classification technique of ENVI software is applied on decomposed outputs, which used a set of training samples from different classes to assign membership values for deriving ground features from three separate components namely double, volume and odd or single bounce. Classified outputs of different decomposed outputs are presented in Figure 6c, 7c, 8c and 9d.

**Results and Analysis**

The analysis of decomposed outputs and classified data results are mentioned in the following sections.

Coherent Decomposition Outputs: Figure 6a and 6b corresponds to the decomposed outputs of Dual pol data. These results are generated using Coherent Decomposition (Pauli and Sinclair) methods considered for the study. This data comprises cultivated area and urban structures (roads). From Figure 6a and 6b, these decomposed outputs prominently represent the natural objects (vegetation) on the ground but urban settlements (roads) in between crop fields are not clearly differentiated from other objects on the ground. The class seperability analysis is performed for the decomposed outputs of Dual pol data which are used for the classification. Classified (SVM) output of decomposed product is presented in Figure 6c.This study has shown that the Coherent decomposition parameters operate on the individual pixels on a coherent basis provides useful information for the land cover classification.

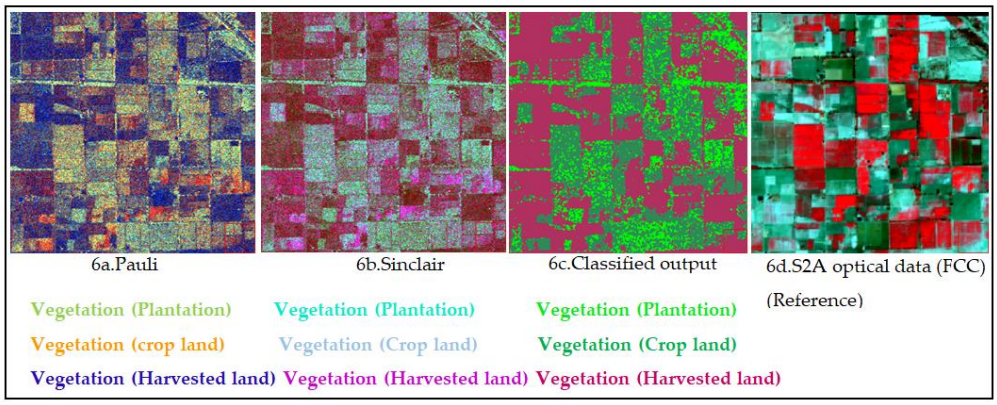


**Fig. 6** Decomposed products, Classified output of Dual pol data and Sentinel-2A data of study area1.

In order to evaluate the classification results, this paper further calculated the confusion matrix, in the two extraction results. Accuracy evaluation as shown in Table1 and 2.

**Table 1** Training samples and selected polygons for study area1.

| Class | Number of Training samples | Number of Polygons |
|---|---|---|
| Crop land | 833 | 2 |
| Harvested land | 809 | 2 |
| Plantation land | 531 | 3 |

**Table 2** Confusion matrix for Sinclair and Pauli classified outputs of Dual pol data.

| Method | Class | Cropland | Harvested land | Harvested Plantation | Precision (%) |
|---|---|---|---|---|---|
| Sinclair | Cropland | 727 | 6 | 100 | 87.27 |
| | Harvested land | 11 | 773 | 25 | 95.55 |
| | Plantation | 50 | 0 | 481 | 90.58 |
| Pauli | Cropland | 743 | 0 | 90 | 89.19 |
| | Harvested land | 5 | 791 | 13 | 97.77 |
| | Plantation | 30 | 0 | 501 | 94.35 |

Overall accuracy = 91.16 %, Kappa = 0.866 for classified Sinclair decomposed output
Overall accuracy =93.65 %, Kappa = 0.904 for classified Pauli decomposed output

*Incoherent Decomposition Outputs:* Figure 7a, 7b, 8a and 8b corresponds to the decomposed outputs of Full-pol data. The decomposed outputs are presented in Figure 7a and 7b generated using Pauli and Freeman-Durden Decomposition methods and the results are presented in Figure 8a and 8b generated using Sinclair and Freeman-Durden Decomposition methods which are considered for this study. The outputs (Figure 7a and 7b) comprise man-made structures, vegetation and waterbody area. The outputs (Figure 8a and 8b) include much of the land surface area is covered by settlements, roads, railway line, lake and cultivated area.

The results from Figure 7a and 8a are shown that, the Coherent decomposition (Pauli and Sinclair) outputs prominently represent the natural objects vegetation and waterbody area but not ideal for highlighting the urban (man-made) structures. This indicates that Coherent decomposition parameters present the most contrast between the natural (land-cover) and urban (land-use) classes representing single bounce is from waterbody, double or even is from urban structures and volume scattering is from forests, respectively. From Figure 7b and 8b, the Freeman-Durden (Incoherent) decomposition method possesses similar characteristics to the Coherence (Pauli) based decomposition, but it is ideal for

highlighting the urban (man-made) objects. Freeman-Durden decomposition method provides a more realistic representation, it discriminates the natural and urban objects separately, because it uses scattering models with dielectric surfaces.

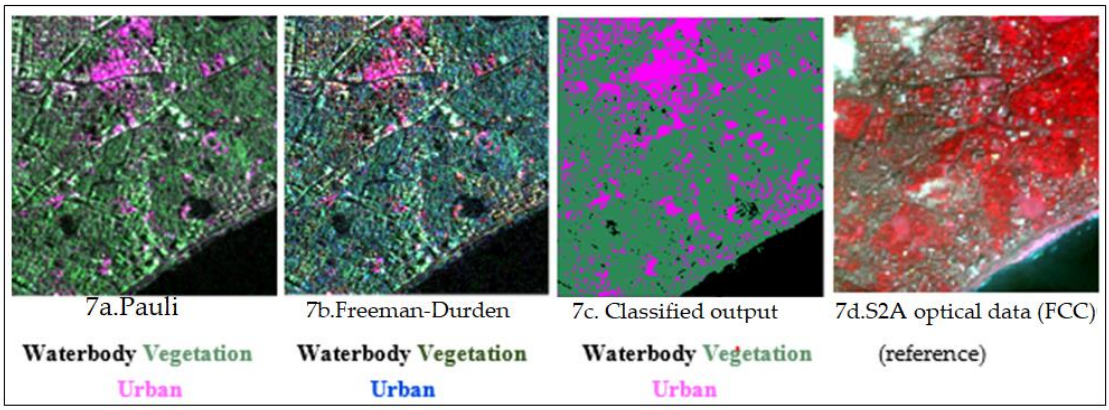


**Fig. 7** Decomposed products, Classified output of Full-pol data and Sentinel-2A data of study area2.

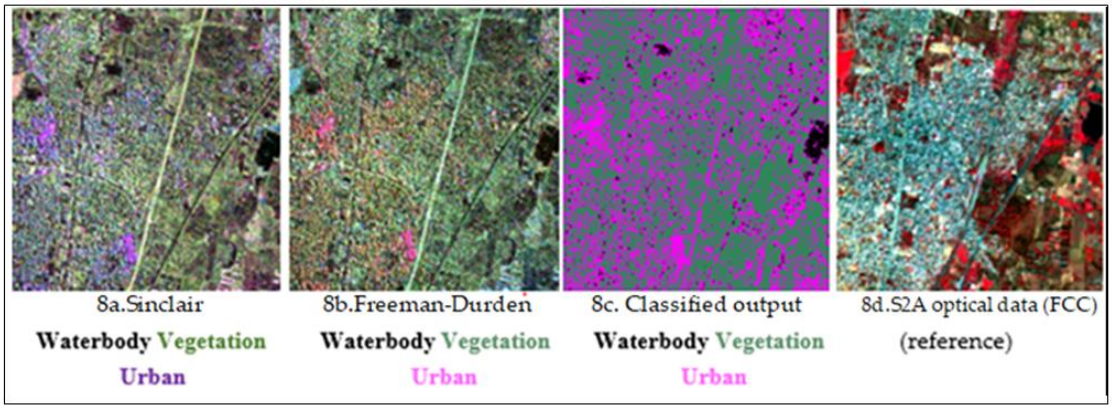


**Fig. 8** Decomposed products, Classified output of Full-pol data and Sentinel-2A data of study area3.

Classified (SVM) outputs of these decomposed outputs are presented in Figure 7c and 8c. This result shows classification accuracy of various features for different scattering mechanisms. The statistical analysis of study area two is mentioned in Table 3 and 4. From the results Figure 7a, 7b, 8a and 8b, it is clearly observed that Freeman-Durden decomposition method gives better accuracy than Pauli and Sinclair methods.

**Table 3** Training samples and selected polygons for study area2.

| Class | Number of Training samples | Number of Polygons |
|---|---|---|
| Crop land | 762 | 2 |
| Harvested land | 1932 | 2 |
| Plantation land | 189 | 3 |

**Table 4** Confusion matrix for Pauli and Freeman-Durden classified outputs of Full-pol data.

| Method | Class | Waterbody | etation | Veg an | Urb | Precision (%) |
|---|---|---|---|---|---|---|
| Pauli | Waterbody | 753 | 9 | 0 | 98.81 | |
| | Vegetation | 4 | 1924 | 4 | 99.58 | |
| | Urban | 0 | 10 | 179 | 94.7 | |
| Freeman-Durden | Waterbody | 743 | 19 | 0 | 97.5 | |
| | Vegetation | 46 | 1876 | 10 | 97.1 | |
| | Urban | 0 | 0 | 189 | 100 | |

Overall accuracy =99.063 %, Kappa = 0.980 for classified Pauli decomposed output
Overall accuracy =96.36 %, Kappa =0.925 for classified Freeman-Durden decomposed output

*Circular Polarization Decomposition Outputs:* Figure 9a, 9b and 9c correspond to the decomposed outputs of Circular pol data. These results are generated using Circular Pol decomposition (M-Delta, M-Chi and M-Alpha) methods. The methods show the scattering power of land use classes in decomposed outputs. The result Figure 9a shows that, yellow color corresponds to the double bounce from built-up areas (buildings), green color corresponds to the volume scattering from vegetation (trees) and blue color corresponds to the surface scattering from water bodies (ocean). Comparing to M-Chi and M-Alpha outputs, M-Delta output shows that double bounce scattering is dominant in built-up area followed by volume scattering. Visual analysis shows that M-Delta has better image visualization than other outputs.

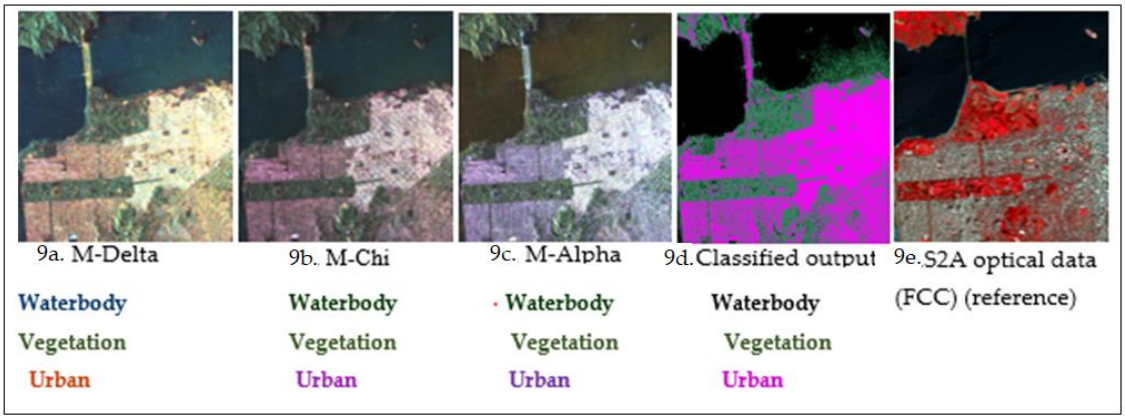


**Fig. 9** Decomposed products, Classified output of Circular pol data and Sentinel-2A data of study area4.

Classified (SVM) output is presented in Figure 9d. Outputs represent that vegetation is more prominent in M-Delta decomposition. This study has shown that volume scattering is produced by vegetation canopy. Comparing the results of M-Chi and M-Alpha, double bounce scattering plays an important role and buildings are prominently in M-Chi output.

**Conclusions**

In this paper the potential of different Polarimetric data of EOS-04 SAR system is addressed to discriminate the land cover classes such as vegetation, water bodies and the land use classes such as buildings, roads that are emphasizing the urban area. Polarimetric SAR data acts as a complementary source of information in planning thematic mapping for management of natural resources. This has been carried-out by Polarimetric decomposition using Circular pol (M-Delta, M-Chi and M-Alpha), Dual pol (Pauli and Sinclair) and Full- pol (Pauli, Sinclair and Freeman-Durden) data in C band. It is observed that Dual pol SAR data accuracy was limited due to its backscattering coefficients had the difficulty to distinguish the return signal from various components of ground objects. But Full-pol data has been used, it can be distinguished various components using decomposition techniques. Freeman-Durden Full-pol decomposition method performed good results in discriminating urban settlements. Circular pol decomposition outputs are showed encouraging results for odd, even and diffused scattering of various features.

Supervised classification (SVM) is classified Polarimetric decomposed outputs into various classes (urban, vegetation and waterbody) based on class rule. SVM classification and Confusion matrices are helped the assessment of available natural and urban settlements for management of natural resources and smart governance. The analysis

carried-out variation of scattering power with respect to density of various man-made structures will be useful for future studies.

**Acknowledgements**
The authors are thankful to Dr. P.V. Radhadevi, Director, ADRIN and Dr. R. Chandrakanth, Deputy Director, SDPAA, ADRIN for their encouragement and support.

**References**

Meng Wang, Changan Liu, Dongrui Han, Fei Wang, Xuehui Hou, Shouzhen Liang and Xueyan Sui, (2022). Assessment of GF3 Full-Polarimetric SAR Data for Dryland Crop Classification with Different Polarimetric Decomposition Methods.

Bikash Ranjan Parida, Shyama Prasad Mandal, (2020). Polarimetric decomposition methods for LULC mapping using ALOS L-band PolSAR data in Western parts of Mizoram, Northeast India.

A. Vyas, V. Nizalapur1, P. Chhasia, D. Rawal1, G. Jain2, A. Das2, (2021), Analysis of different polarimetric decomposition techniques using compact polarimetric NISAR data for Ahmedabad, India.

Shatakshi Verma, Shashi Kumar, and Hamish Dsouza, (2022), Polarimetric Decomposition and Machine Learning-Based Classification of L and S-Band Airborne SAR (LS-ASAR) Data.

Wentao An, Yi Cui, and Jian Yang, Senior Member, IEEE, (2010), Three-Component Model-Based Decomposition for Polarimetric SAR Data.

Katharina Harfenmeister, Sibylle Itzerott, Cornelia Weltzien, Daniel Spengler, (2021), Agricultural Monitoring Using Polarimetric Decomposition Parameters of Sentinel-1 Data.

Şevket Demirci, Caner Özdemir, (2021), An investigation of the performances of polarimetric target decompositions using GBSAR imaging.

Jose Manuel Delgado Blasco. Magdalena Fitrzyk, Jolanda Patruno, Antonio Miguel Ruiz-Annenteros. Mattia Marconcini (2020) Effects on the Double Bounce Detection in Urban Areas Based SAR Polarimetric Characteristics

Hongquan Wang, Ramata Magagi, Kalifa Goita, Thomas Jagdhuber and Irena Hajnsek, (2016), Evaluation of Simplified Polarimetric Decomposition for Soil Moisture Retrieval over Vegetated Agricultural Fields.

Sang-Hoon Hong, Hyun-Ok Kim, Shimon Wdowinski and Emanuelle Feliciano, (2015), Evaluation of Polarimetric SAR Decomposition for Classifying Wetland Vegetation Types.

Balakrishna Penta, A.O. Varghese, K. Nageswara Rao and A.K. Joshi, (2013), Analysis of Synthetic Aperture Radar polarimetric decomposition methods for land cover interpretation.

Sang-Hoon Hong. Member IEEE and Shimon Wdowinski, (2014). Double-Bounce Component in Cross-Polarimetric SAR from a new scattering Target Decomposition.

Deliang Xiang, (2016), Urban Area Information Extraction from Polarimetric SAR Data.

Deliang Xiang, Tao Tang, Canbin Hu, Qinghui Fan, (2016), Built-up Area Extraction from PolSAR Imagery with Model-Based Decomposition and Polarimetric Coherence.

Kiran Dasari, Anjaneyulu Lokam, (2018), Exploring the Capability of Compact Polarimetric (Hybrid Pol) C Band RISAT-1 Data for Land Cover Classification.

Zou, Bin, Lu, Da, Wu, Zhilu, Qiao, Zhijun G, (2016), Urban-area extraction from polarimetric SAR image using combination of target decomposition and orientation angle.

Bhoonidhi URL: https://bhoonidhi.nrsc.gov.in ISRO Open Data Access web application.

**Citation**

Srivally, M.V., Ghosh, S., Chaubey, N., Upadhyay, S., Pandey, S. (2024). Analysis of Different SAR Polarimetric Decomposition Methods using EOS-04 Polarimetric Data for Urban and Natural Features. In: Dandabathula, G., Bera, A.K., Rao, S.S., Srivastav, S.K. (Eds.), Proceedings of the 43rd INCA International Conference, Jodhpur, 06–08 November 2023, pp. 449–459, ISBN 978-93-341-2277-0.